The observation and evaluation of extensional filament deformation and breakup profiles for Non Newtonian fluids using a high strain rate double piston apparatus

M.R. Mackley , S.A. Butler , S. Huxley , N.M. Reis , A.I. Barbosa , M Tembely

PII: S0377-0257(16)30148-3
DOI: 10.1016/j.jnnfm.2016.11.009
Reference: JNNFM 3849

To appear in: *Journal of Non-Newtonian Fluid Mechanics*

Received date: 16 August 2016
Revised date: 15 November 2016
Accepted date: 16 November 2016

Please cite this article as: M.R. Mackley , S.A. Butler , S. Huxley , N.M. Reis , A.I. Barbosa , M Tembely , The observation and evaluation of extensional filament deformation and breakup profiles for Non Newtonian fluids using a high strain rate double piston apparatus, *Journal of Non-Newtonian Fluid Mechanics* (2016), doi: 10.1016/j.jnnfm.2016.11.009

Highlights

- A new fast filament stretching apparatus
- Capable of extensional strain rates exceeding 1000 s^{-1}
- Range of fluids tested
- Deformation and breakup profiles reported
- Some matching of experimental profiles with numerical simulation

The observation and evaluation of extensional filament deformation and breakup profiles for Non Newtonian fluids using a high strain rate double piston apparatus.

by,

M.R.Mackley*, and S.A.Butler
Department of Chemical Engineering and Biotechnology, University of Cambridge, CB2 3RA, UK

S. Huxley
Huxley Bertram Engineering Ltd,
Waterbeach. Cambridge CB25 9QP, UK

N.M.Reis and A.I. Barbosa
Department of Chemical Engineering, Loughborough University
Loughborough, LE11 3TU UK

M Tembely
Department of Mechanical and Industrial Engineering
Concordia University, Montreal. Canada H3G 1M8

Corresponding author* 44 1223 334777 Fax 44 1223 334796 mrm5@cam.ac.uk

***Summary**:*

This paper reports a new design of experimental double piston filament stretching apparatus that can stretch fluids to very high extensional strain rates. Using high speed photography, filament deformation and breakup profiles of a strategically selected range of fluids including low and higher viscosity Newtonian liquids together with a viscoelastic polymer solution, biological and yield stress fluids were tested for the first time at extensional strain rates in excess of 1000 s^{-1} . The stretching rate was sufficiently high that observation of low viscosity Newtonian fluid stretching, end pinching and break was observed during the stretching period of the deformation, whereas for a higher Newtonian viscosity, filament thinning and breakup occurred after the cessation of piston movement. Different fluid rheologies resulted in very different thinning and breakup profiles and the kinetics, in particular of yield stress fluids showed a striking contrast to Newtonians or viscoelastic fluids. Surprisingly all the tested fluids had an initial sub millisecond "wine glass" profile of deformation which could be approximately captured using a simple parabolic mass balance equation. Subsequent deformation profiles were however very sensitive to the rheology of the test fluid and where the final breakup occurred before or after piston cessation. In certain cases the thinning and break up was successfully matched with a 1D numerical simulation demonstrating the way numerical modelling can be used with the fluids correct rheological characterization to gain physical insight into how rheologically complex fluids deform and breakup at very high extensional deformation rates.

Key words: High extensional strain rates; Filament deformation profiles; Filament break up; Filament stretching; polymer solutions; biological and yield stress fluids.

1. Introduction.

This paper is concerned with the development of a fast strain rate filament stretching device that can stretch fluids at strain rates in excess of $1000s^{-1}$ and thereby enables low viscosity and other fluids to be observed during fast filament extensional stretching. A scientific objective of the paper is to observe and understand how a range of different fluids deform and breakup under extreme extensional conditions. There is an extensive literature on extensional stretching devices, however in the past these have been essentially universally used to obtain rheological extensional viscosity data on fluids with a base viscosity higher than 1Pas, either from coupled force extension observations during stretching [1] or filament thinning data during filament relaxation after stretching [2]. The extensional droplet breakup of Newtonian and Non Newtonian droplets has also been extensively studied, James et al [3] and review [4], however again most experimental observations have generally been limited to high viscosity fluids.

Obtaining high extensional strain rates is a challenging problem and many devices that achieve this involve high velocity jet flow or confined constriction flow which can contain upstream simple shear components in addition to extensional deformation [5,6]. Low viscosity viscoelastic polymer solutions are particularly challenging in extensional flow because viscoelastic effects can be expected to occur when both the fluid Weissenberg $We = \lambda\,\dot{\varepsilon}$ number is greater than one and when the total strain is high, where λ, is the relaxation time and $\dot{\varepsilon}$ the strain rate (Crowley et al [7]) . For a dilute polymer or biological solution λ might be of order 10^{-3} s or less which means for $We > 1$, the extensional strain rate needs to exceed 10^{3} s^{-1}. In addition, chain stretching may be necessary to induce a rheology change or changes in deformation profiles and so there is an added strain requirement that $\gamma \gg 1$. These conditions greatly constrain experimental configurations for this type of deformation at high strain rates. The double jet apparatus (Mackley et al [8]) was specifically developed for high *We* extensional flow and although the apparatus was successful in optically detecting localised chain stretching it was not particularly effective as a rheometer and was a closed system so that free surface deformation profiles could not be observed.

In the past, essentially pure extensional filament stretching using one moving opposed piston and coupled force measurements has been successfully used for reasonably high viscosity Newtonian and polymer based fluids (see for example reviews by Anna et al [1], and McKinley et al [9], where fluids investigated had viscosities typically greater than 1 Pas. In this class of experiment the key objective was to extract rheological extensional viscosity parameters. The idea of using capillary thinning after stretching as an additional way of determining the extensional viscosities of structured fluids was introduced by Bazilevsky et al [10] who developed a device that involved the stretching of a fluid filament and then following the subsequent time evolution of surface tension driven capillary thinning, where again in general but not exclusively, high viscosity fluids were used (see for example reviews by Anna et al [11], McKinley [2]). In general these filament thinning experiments were carried out without the necessity of force measurement and both extensional viscosity and relaxation times of Non Newtonian fluids could be extracted from the data. A key finding of the extensive filament thinning experiments that have been carried out was that Newtonian fluid centre line thinning occurred with a linear decay and viscoelastic fluids with an exponential decay, see for example, [12,13,14,15]. For essentially all the cases of extensional filament thinning and breakup studied, data was obtained after the initial stretch process was complete.

A related experiment to extensional filament stretching is gravity driven drop filament thinning (see for example, Cooper-White et al[16]) where both high and low viscosity Newtonian and Non Newtonian fluids have been studied for many decades. These experiments provide

essentially constant external force boundary conditions and provide a useful way of observing extensional break up.

The apparatus developed in this paper was specifically designed to study the high strain rate deformation and breakup of initially low viscosity Non Newtonian ink jet fluids where the behaviour of ink jet fluids emerging from nozzles is of critical importance for ink jet performance, see for example [17]. The problem is however of general scientific and technological importance as droplet stretching and breakup of in particular low viscosity fluids, pervades many industrial and natural processes such as ink jet and spray technology together with silk worm and spider spinning . Up until the development of the apparatus described in this paper there was no piston device that was capable of the controlled high speed stretching of fluids where optical observations could be conveniently and systematically recorded.

The general experimental deformation geometry for most filament stretching and thinning devices are shown schematically in Figure 1 where fluid is initially positioned between two pistons with diameter D at a starting gap of L_0 (Figure 1a). Either one or both pistons are then moved at a constant speed V_p and stretching takes place (Figure 1b). During this period, provided force measurements are carried out, it is possible to determine the transient extensional viscosity of the fluid using information on the capillary thinning at the centre of the filament, See for example [9]. Subsequently when the pistons stop moving (Figure 1c), capillary thinning can take place due to surface tension forces and it is possible to derive a transient viscosity from this thinning action without the need to make force measurements. See for example Anna et al [11], Clasen et al [14]. Both the stretch and relaxation behaviour of Newtonian and viscoelastic fluids have been successfully modelled and simulated for high viscosity fluids. (see for example, Yao et al [15] and Vadillo et al [18]).

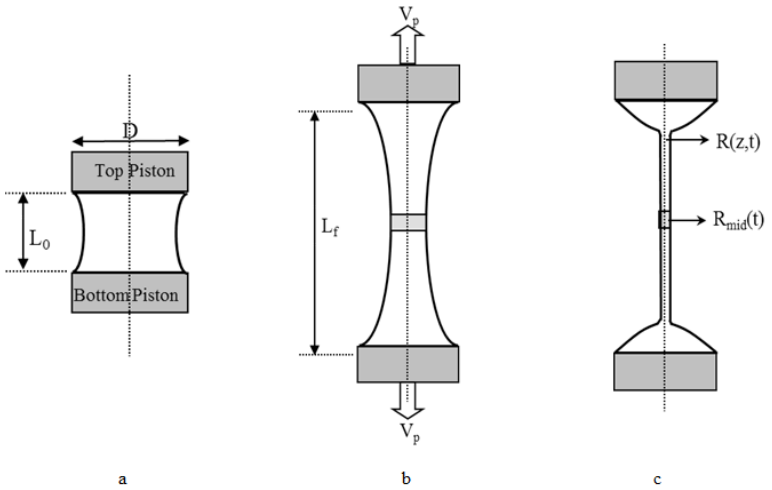

***Figure 1**. Schematic diagram showing, **a)** initial conditions, **b)** filament stretching and **c)** filament thinning.*

.

One of the only commercial filament stretch and thinning apparatus currently available is the Caber Apparatus (http://www.thermoscientific.com/content/tfs/en/product/haake-caber-1-capillary-breakup-extensional-rheometer.html) and extensional viscosity results using this device are reported for example by Rodd et al [19]and Clasen et al [14]. The manufacturers of the Caber quote a maximum stretch rate for the apparatus of order 3 s^{-1} and typically during the subsequent filament thinning stage the extensional strain rate is of order 10 s^{-1}. An alternative to the Caber instrument is the Trimaster series developed at the University of Cambridge (Vadillo et al [20]). The device has two pistons that move in opposite directions thereby keeping the centre of the filament in the same central position and the maximum useful achievable stretching strain rate that can be obtained without excessive overshoot is of order 12 s^{-1}. In order to extend the strain rate range of the Trimaster a new Huxley Bertram (HB4) Cambridge Trimaster has been developed that uses a unique method of achieving high strain rate extensional piston movement. This paper describes the mechanical principle and performance of the apparatus and presents extensional

deformation and breakup profiles for Newtonian fluids, a viscoelastic solution and a selection of other potentially rheologically complex fluids. The paper also matches some thinning and breakup results with analytic equations and a numerical simulation.

2. The development of the Huxley Bertram (HB4) Trimaster series apparatus

A schematic diagram of the HB4 fast filament stretching apparatus is shown in figure 2a and a photograph of the apparatus is given in figure 2b. The apparatus is designed around the principle of achieving the highest possible double piston separation velocity in order to obtain stretching strain rates greater than 1000 s^{-1}. This involves moving two mutually opposed pistons from rest as quickly as possible. Piston movement is achieved by the movement of two lever arms shown in Figure 2a.and the movement of the lever arms are activated by ramps that are positioned on a separate horizontal wheel. The purpose of the wheel is to allow a servo motor that drives the wheel to accelerate the wheel to its maximum velocity before the ramp starts to move the lever arms and piston. In this way the inevitable finite start up inertia of the servo motor and wheel is overcome and the required high velocity of the piston pin achieved within sub milliseconds.

As shown in figures 2a and 2b, two mutually opposed vertical piston pins are mounted within guide blocks. The piston pins are mounted within the fixed guide block so that they can only move vertically and there is light friction in the guides in order that whilst at rest, pistons do not move under gravity. There is a head at the top of each piston pin and the underside of these heads touches a lifter block on each of two horizontal lever arms. The two stiff but light horizontal lever arms are pivoted at one end and the other end carries hardened steel rollers. These rollers can be moved vertically by a hardened steel ramp which is positioned on the periphery of a light horizontal wheel driven by a vertically mounted servo motor (type SGMAH 08A from Omron Electronics Ltd). The hardened steel ramp (consisting of a ramp up, level section and ramp down section) is attached to the periphery wheel and covers some 30 degrees of rotation of the wheel. This means the wheel can start turning from a position some 300 degrees before the ramps makes contact with the rollers on the pivot arms. This allows the servo motor to accelerate the wheel up to the required peripheral velocity of up to 6 m s^{-1} before the ramp contacts the rollers. At the start of an experimental test the piston pin heads touch the lift blocks on the lever arms which are positioned so the working ends of the piston pins are at the required initial separation. In this position the rollers are clear of the periphery of the wheel and both pistons will subsequently be driven apart at the required amount by the ramped section of the wheel. The wheel accelerates up to speed and then the ramp passes between the rollers, giving them a separation velocity which is transmitted via the lift blocks to the piston pins. Both pins move simultaneously and in an opposite direction thereby ensuring the centre of field of view remains constant. After the ramp has passed the rollers, the arms return to their original position but the friction in the guide blocks holds the piston pins at the end position. Stops are positioned to prevent over-travel of both the arms and piston pins.

The ms movement of piston pins and the requirement for them to have some intrinsic friction means that it is unrealistic to include a force transducer in either one or both of the piston pins. The apparatus is therefore limited to optical interrogation of the resulting deformation and breakup profile for the small fluid samples initially positioned between the piston gap. In addition, the complex mechanical arrangement of the HB4 does not lend itself easily to temperature control and all results reported in this paper were carried out at room temperature.

Figure 2c shows as series of amplitude *vs* time traces obtained by following the piston displacement using a high speed camera (type Photron Fastcam 1024PCI, model 100k @18,000 frames/s with a resolution of 128x256 pixels) which is attached to the HB4 apparatus. The data demonstrates that when the piston is moving for individual piston velocities above 0.1 m s^{-1}, the piston velocity is reasonably linear and on cessation of piston movement there is relatively little overshoot and subsequently the position of the pistons remains constant. The low velocity piston

trace at 0.1 m s^{-1} does show a small non-linear response believed to originate from a beam resonance effect. For all experiments carried out in this paper vertical piston velocities of 0.5 m s^{-1} were used giving a combined piston separation speed of 1.0 m s^{-1}. For fluid testing a Reynolds number of $= \rho\, v\, d/\eta$, where ρ is density, v velocity, d a length and η viscosity, is of order 10^3 for the low viscosity 1.0 mPas fluids tested, which is well into the inertial regime for fluid filament stretching experiments. When combined separation velocities greater than of order 3 m/s were used there was some overshoot of the pistons and for low viscosity fluids the appearance of transient waves could be seen on the early stages of the deformation profile development; this feature however was not observed for any of the fluid tests reported in this paper. The apparatus operates at ambient temperature and all experiments reported in this paper were carried out at 22^0 C.

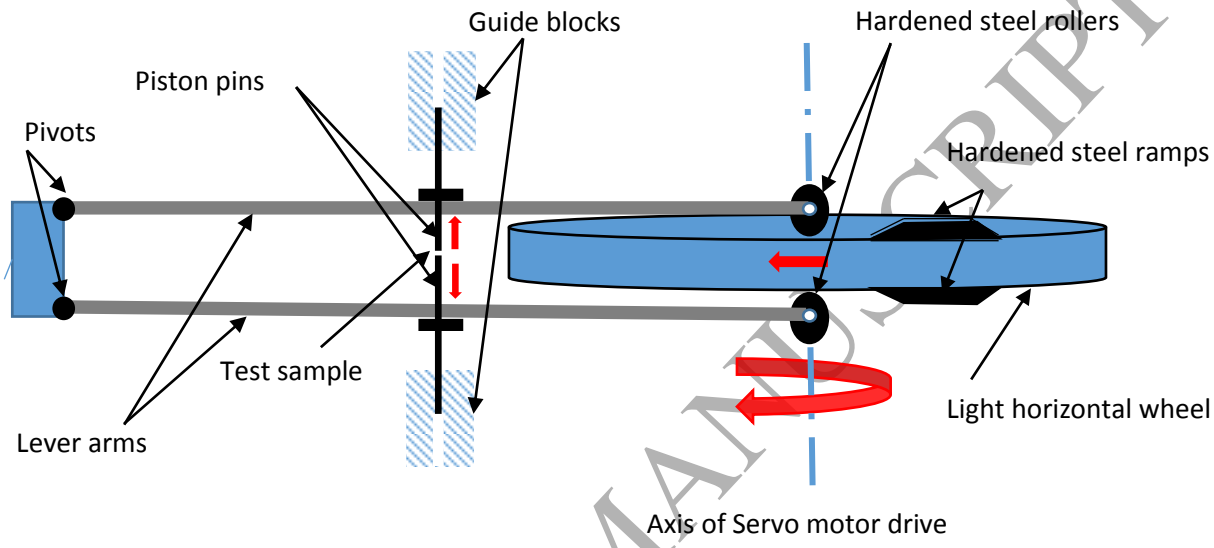

2a

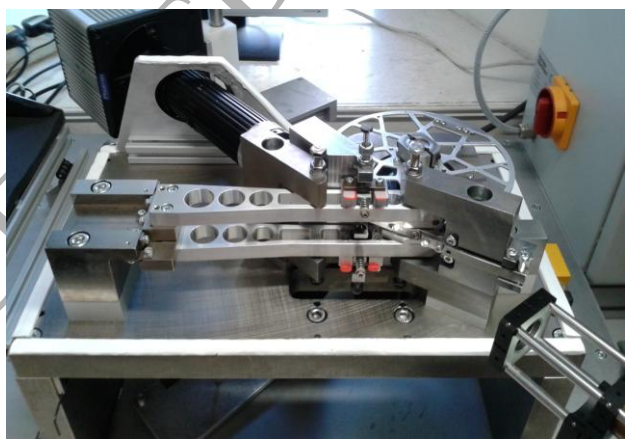

2b

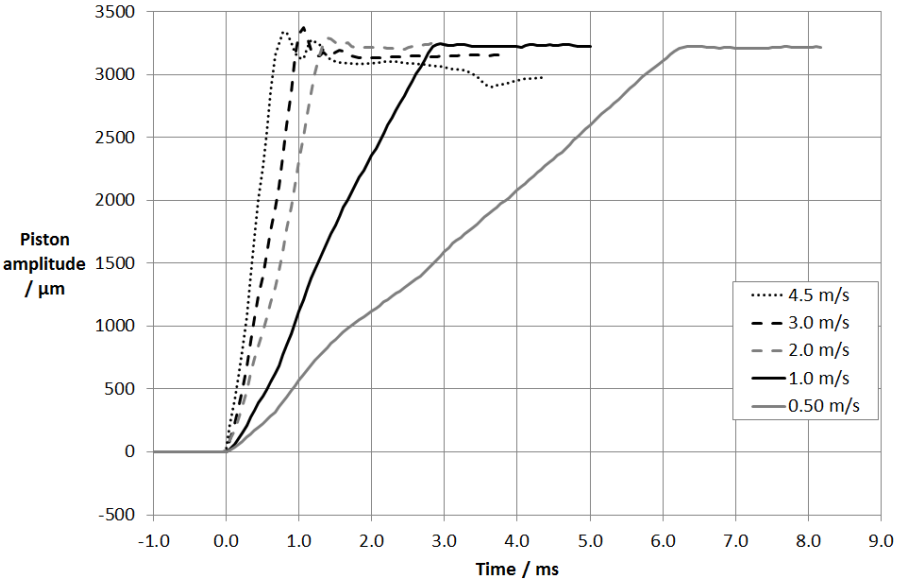

2c

Figure 2. a) *Schematic diagram of HB4 Cambridge Trimaster.* ***b)*** *Photograph of HB4.* ***c)*** *Plot of combined piston displacement as a function of time for different combined piston speeds.*

3. Experimental evaluation of test fluids

In order to evaluate the performance of the HB4, a series of experiments were carried out on different fluids and some of these are reported below. In each of the reported cases stainless steel pistons of D = 1.2mm diameter were used at a chosen combined separation speed of 1.0 m s^{-1}. Piston diameter, piston travel and piston velocity can all be changed on the HB4; however in order to aid comparison with different fluid rheology these variables have been kept constant in this paper. At the start of each experiment the pistons are positioned with a set starting gap of order L_0 = 0.35 mm and the test fluid was then micro pipetted or placed into the gap with a spatula depending on viscosity and any excess fluid removed from the pistons using paper tissue. The starting condition is then essentially a cylinder of fluid attached to both pistons. In all cases tested, during stretching the fluids remained in contact with the pistons over their entire diameter.

The following strategic choice of fluids were chosen for testing.

- **Newtonian fluids.** A Brookfield calibration Newtonian silicon oil of viscosity 492 mPas was used as a relatively high viscosity fluid that gave a representative response for this and higher Newtonian viscosities. A low viscosity Newtonian Phosphate Buffer Solution (Dubelco's PBS) with a viscosity of 1.03 mPas was also used as a representative low viscosity watery fluid and one that is extensively present in biological formulations.
- **Polymer solution.** A 1% w/w monodisperse (110K MW) polystyrene solution in diethyl phthalate was used (viscosity 15.3 mPas and surface tension 37 mN/m) as a representative low viscosity viscoelastic polymer solution and where the linear viscoelastic and shear rheology together with its lower strain rate extensional deformation profile has been given in previous publications (Vadillo et al [18], [20]).
- **Protein Solutions**. A range of protein solutions including egg white and yolk were chosen as these had not been tested before at high extensional strain rates. It was hoped that chain stretching effects might be observed at the high strain rates for some of the biological fluids tested. The egg white proved to be particularly useful as progressive dilution enabled a transition from that of a viscoelastic polymer solution to a low viscosity Newtonian response to be followed.
- **Yield stress fluids**. No previous work appears to have been carried out on the high strain rate extensional behaviour of yield stress fluids and two well-known brands of thickened sauces were selected as being universally readily available test fluids.

3.1 Newtonian fluids.

In order to provide a reference to previous lower strain rate experiments, a Brookfield Silicone oil standard was initially selected; where the oil has a Newtonian viscosity of 492 mPas and a surface tension of 22.5 mN/m. Experiments were carried out at the combined piston separation speed of 1m/s. Figure 3 shows both a photographic time evolution of the overall observed deformation profile and also a graph of piston displacement and experimentally measured centre line time evolution. In this particular case the viscosity of the fluid was sufficiently high for a stable filament to exist at the end of the piston movement and surface tension driven capillary thinning continued to occur throughout the 25 ms of recorded data. During the early deformation period the deformation profile takes the form of a symmetric "wineglass" appearance, then during the later cessation period, a filament forms between the stationary pistons and thins with a linear decay in a similar way to other high viscosity Newtonian fluids reported for similar previous experiments carried out a lower initial stretching rates. (See for example by Liang et al [13] and McKinley [2]).

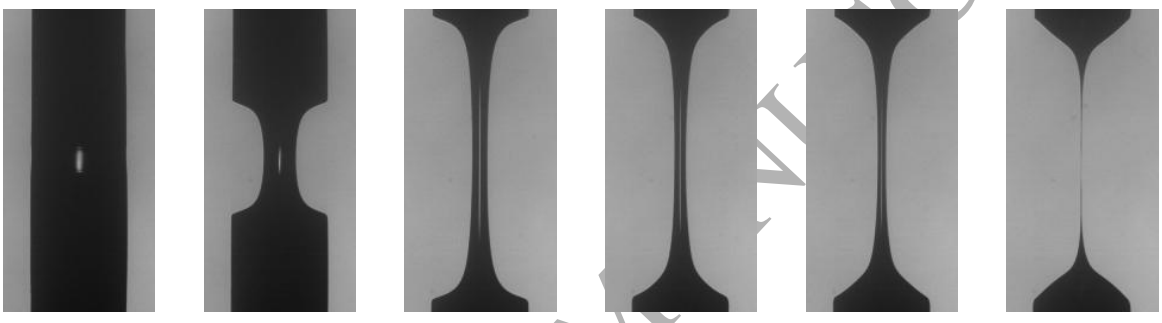

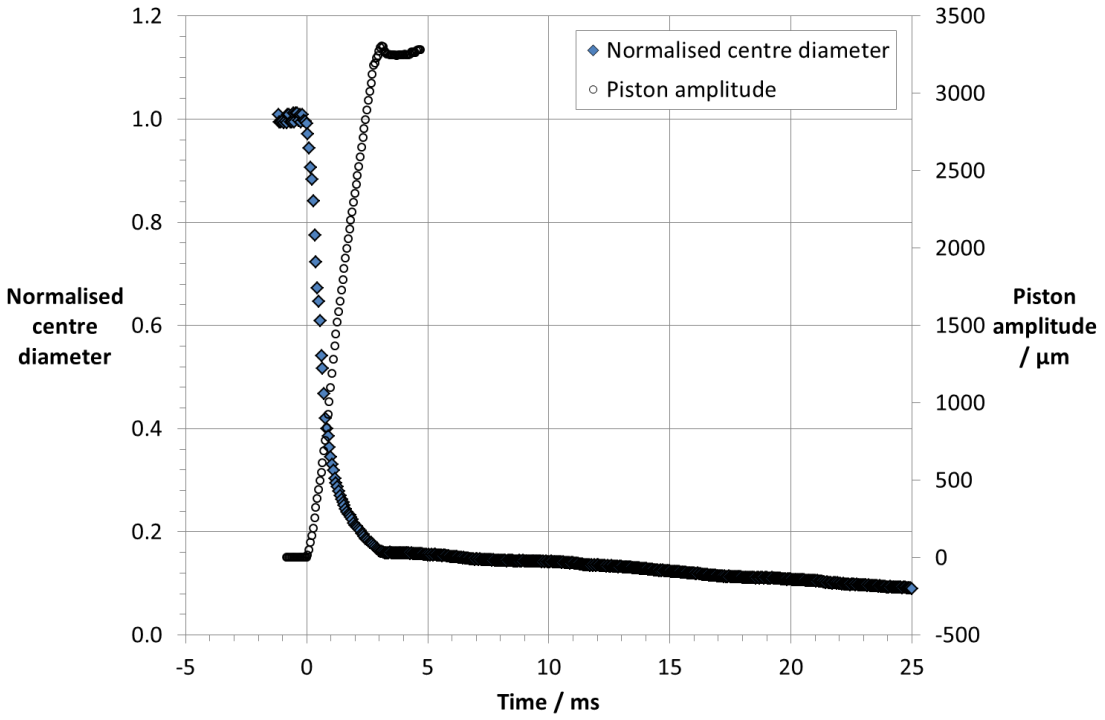

Figure 3. *Photographs for a Newtonian Brookfield calibration silicone oil. The graph shows normalised centre filament diameter and piston amplitude as a function of time. Piston diameter =1.2mm, initial gap = 0.35mm, combined separation speed = 1 ms^{-1}*

Deformation profiles are sensitive to base viscosity and this is shown by comparing the behaviour described in figure 3 with the results for a low viscosity Newtonian fluid shown in figure 4. In figure 4 a Newtonian Phosphate Buffer Solution (Dubelco's PBS) was used and the solution has a room temperature viscosity of 1.03 mPas with a surface tension of 69.5 mN m^{-1}. The photographic deformation profile in Figure 4 shows significant differences to figure 3. Initially, in a similar way to the higher viscosity silicon oil, The low viscosity buffer solution starts deforming through a "wineglass" deformation profile, however in this case the break up of the buffer filament happens during the deformation stage of the piston movement and also breakup occurs by "end pinching" of the fluid. The form of end pinch breakup is similar to that reported for lower extensional strain rate deformation of low viscosity Newtonian fluids (Vadillo et al [20]); but at the lower strain rates reported by Vadillo et al, the end pinching occurred during the stationary piston period after piston movement had stopped.

Figure 4 also shows the displacement profile for a period of 2ms and during this time the center diameter ratio of the fluid decreases as shown in the figure. From this measurement it is possible to calculate both the instantaneous strain rate $\dot{\gamma}$ and Hencky strain ε of the deformation from the following equations.

$$\dot{\varepsilon} = -2\,\frac{1}{D}\,\frac{dD}{dt} \qquad \varepsilon = \int \dot{\gamma} dt = -2\int \frac{dD}{D} = 2\,ln\frac{D_0}{D} \quad \ldots\ldots (1)$$

Figure 4 shows that for this Newtonian buffer solution, the extensional strain rate varies from of order 3500 s^{-1} at the start of the deformation to 1000 s^{-1} after 2ms. During this time the Hencky strain progressively increases to ~3.5 and the data confirms that the HB4 achieves both very high strain rates and Hencky strains during the stretch period of the piston movement. During the short piston displacement period, the order of magnitude stretch strain rates and Hencky strains observed for the buffer were also of a similar order of magnitude for all of the remaining fluids described in this paper. Inevitably both strain rate and strain will vary during the test; however the order of magnitude in strain rate is a least a decade greater than any other piston operated device.

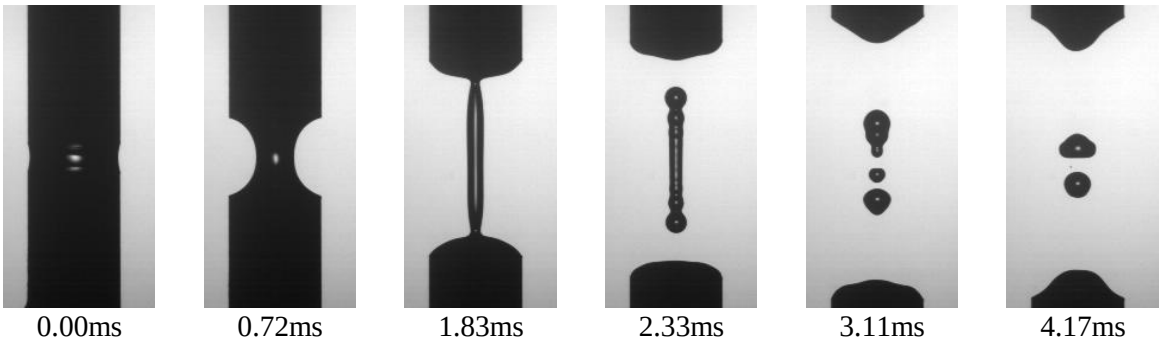

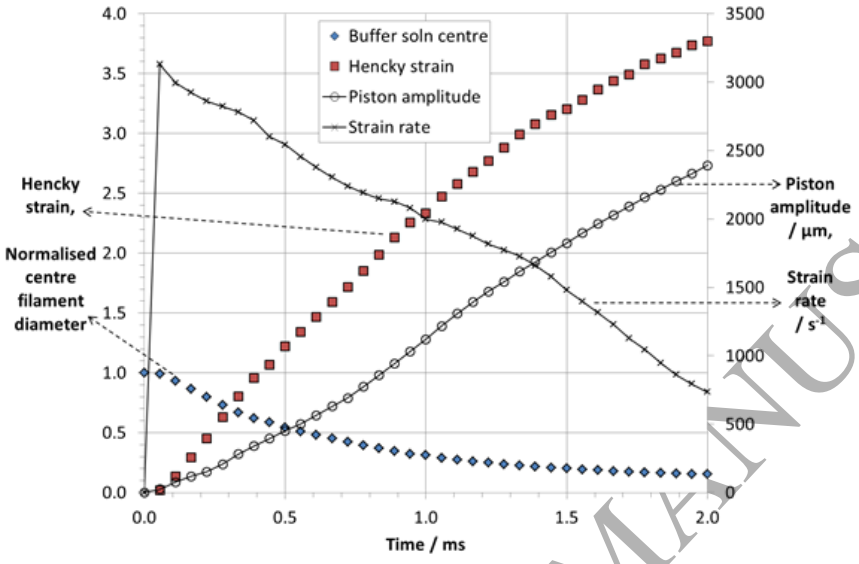

Figure 4. *Photographs for a Newtonian PBS buffer. The graph shows Hencky strain, Normalised centre filament diameter, piston amplitude and centre line strain rate plotted as a function of time. Piston diameter = 1.2mm, initial gap = 0.35 mm, combined separation speed = 1 ms^{-1}.*

3.2. Monodisperse Polystyrene solution.

A 1 weight % monodisperse (110K MW) polystyrene solution in diethyl phthalate was used (viscosity 15.3 mPas and surface tension 37 mN/m) as a representative low viscosity polymer solution and the rheology together with its lower strain rate extensional deformation profile has been given in a previous publication (Vadillo et al [18], [20]). In the case of the polymer solution, the early stage wine glass thinning process shown in Figure 5 appears similar to both the previous Newtonian engine oil and buffer solution, however at longer times, a more stable and longer lasting filament is formed when compared with the buffer solution and filament breakage occurs after the cessation of piston movement with very much less pronounced end pinching than the buffer solution. The thinning process seen in the photographs and also the figure for both center and minimum thickness diameter, carries on well after the pistons have stopped moving and this compares in a similar way to the same fluid testing reported in (Vadillo et al [20]) using the lower strain rate Mk2 Trimaster apparatus. Final break up can occur at a number of different positions along the thin filament and can vary in position for different runs under the same initial boundary conditions. The results show that the deformation profile for the polymer solution is different to that of the Newtonian low viscosity buffer case and the higher Newtonian viscosity silicon oil.

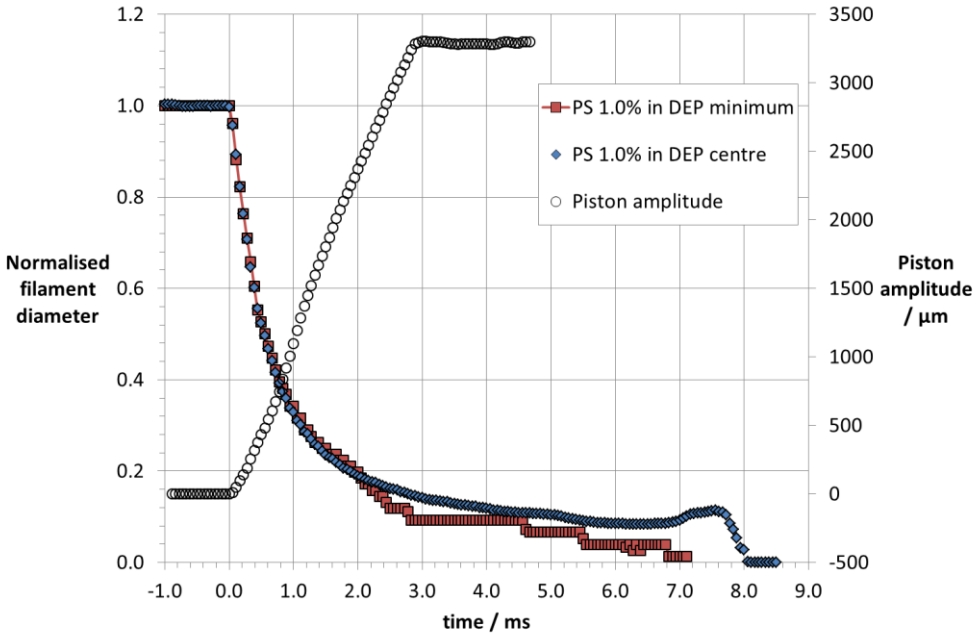

***Figure 5**. Photographs, displacement, centre line and minimum thickness plots for a 1wt% solution of polystyrene (MWt =110,000) in diethyl phthalate. Piston diameter = 1.2mm, initial gap = 0.35 mm, combined separation speed = 1 m s^{-1}.*

3.3 Protein solutions

Proteins are polymeric and might be expected to behave differently to Newtonian fluids during high strain rate stretching and in order to evaluate behaviour, a range of different protein containing fluids were examined. Both hen egg white and yolk were examined, together with the purified and hydrolysed proteins albumin and lysozyme dilutes in PBS buffer. Egg white consists of a mixture of several proteins (albumins, mucoproteins and globulins) dissolved in 90% v/v water. The rheology of egg white, including some low deformation rate filament stretching results has recently been studied by Cardinaels et al [21]. Early work on egg white shear thinning (Tung et al [22]) considered egg white albumen as a single phase, however others, such as Kemps et al [23] and Cardinaels et al [21] considered the "thick" and "thin" components of egg white separately. Egg white contains both soluble and insoluble egg proteins in an aqueous medium (Shenstone [24]), whereas egg yolk consists of protein granules suspended in aqueous plasma (Huopalahti [25]) and shear thinning rheology of egg yolk has been reported by Telis-Romero et al [26]. Both albumin and lysozyme are natural proteins that are present in eggs. Albumin is also the main protein in human and bovine blood plasma and has a relative molecular weight of 67-70 Dalton, lysozyme has a lower molecular weight of 14 kDalton.

Examples of the behaviour of both unpurified egg white and egg yolk are shown in Figure 6. A fresh, free range one day old egg was separated into its white and yolk components and in

these experiments the egg white was treated as a single phase. The HB4 results shown in Figure 6 indicate that the egg yolk and white behave in very different ways when stretched at a high extensional strain rate. Both the egg white and egg yolk initially thin to form the now familiar wineglass geometry, however subsequent behaviour is markedly different. In the case of the egg white, a long living thin thread is formed which finally breaks some 100 ms after stretching. The thinning behaviour is reminiscent of a high molecular synthetic polymer of the type reported in this paper and also for example in Vadillo et al [20].

The egg yolk showed a quite different behaviour to any of the other fluids that had been described so far. Thinning and break up occurred during stretching and "ductile fracture" occurred without end pinching during the stretching period. After ductile fracture there was a partial retraction of the remaining fluid attached to each piston. This behaviour is different to Newtonian and polymer behaviour and seems to be the type of behaviour expected from a fluid with a yield stress. Niedzwiedz et al [27] have used low strain rate Caber filament thinning data to obtain yield stress measurements for concentrated emulsions and these could now be complemented by HB4 high shear rate filament stretch behaviour of the type observed for the egg yolk.

Figure 7 shows the effect of buffer solution dilution for egg white and it is only when the dilution levels reach around 64:1 volume ratio that a base, low viscosity Newtonian behaviour is recovered. At low dilutions the thinning behaviour remains polymeric in appearance. The time dependence of the filament decay is shown in greater clarity in Figure 8 where the minimum thickness is plotted as a function of time and the decay time progressively decreases with increasing dilution. The figure shows clearly that for high strain rate deformation, the progressive transition from a polymeric filament thinning deformation profile to that of a low viscosity Newtonian fluid can be followed using the HB4. The figure also shows the transition for filament break up, that at full concentration occurs after the cessation of piston movement whereas at high dilution, break up occurs during the initial piston movement.

The behaviour of two purified protein polymers in PBS buffer are shown in Figure 9. The 50% w/w lyophilised albumin from chicken egg solution showed some sign of polymeric behaviour with slightly longer decay times than a Newtonian fluid and a thin filament tails, whilst the 50 mg/ml lysozyme solution (prepared from chicken egg powder supplied by Sigma Aldrich), showed an essentially classic low viscosity Newtonian behaviour. The Newtonian steady shear viscosity of the albumin solution was 64 mPas and the lysozyme solution was 1.5 mPas and so some of the difference in the two decay behaviour might be attributed to base viscosity differences alone. These findings however differ considerably from other lower shear rate surface and bulk rheology simple shear data for both albumin and lysozyme where significant viscoelastic effects were discovered at low shear and associated with strong protein aggregation at an air/water interface to create a viscoelastic film while the interior of the solution was Newtonian (Sharma et al [28], Castellanos et al [29]. Presumably in the case of the HB4 high shear rate extensional experiments the deformation rates are presumably sufficiently high for surface viscoelastic effects not to play a significant part in the deformation and the observed HB4 near Newtonian response suggests that in both cases, HB4 polymer chain stretching did not take place to change the overall rheology of the fluid.

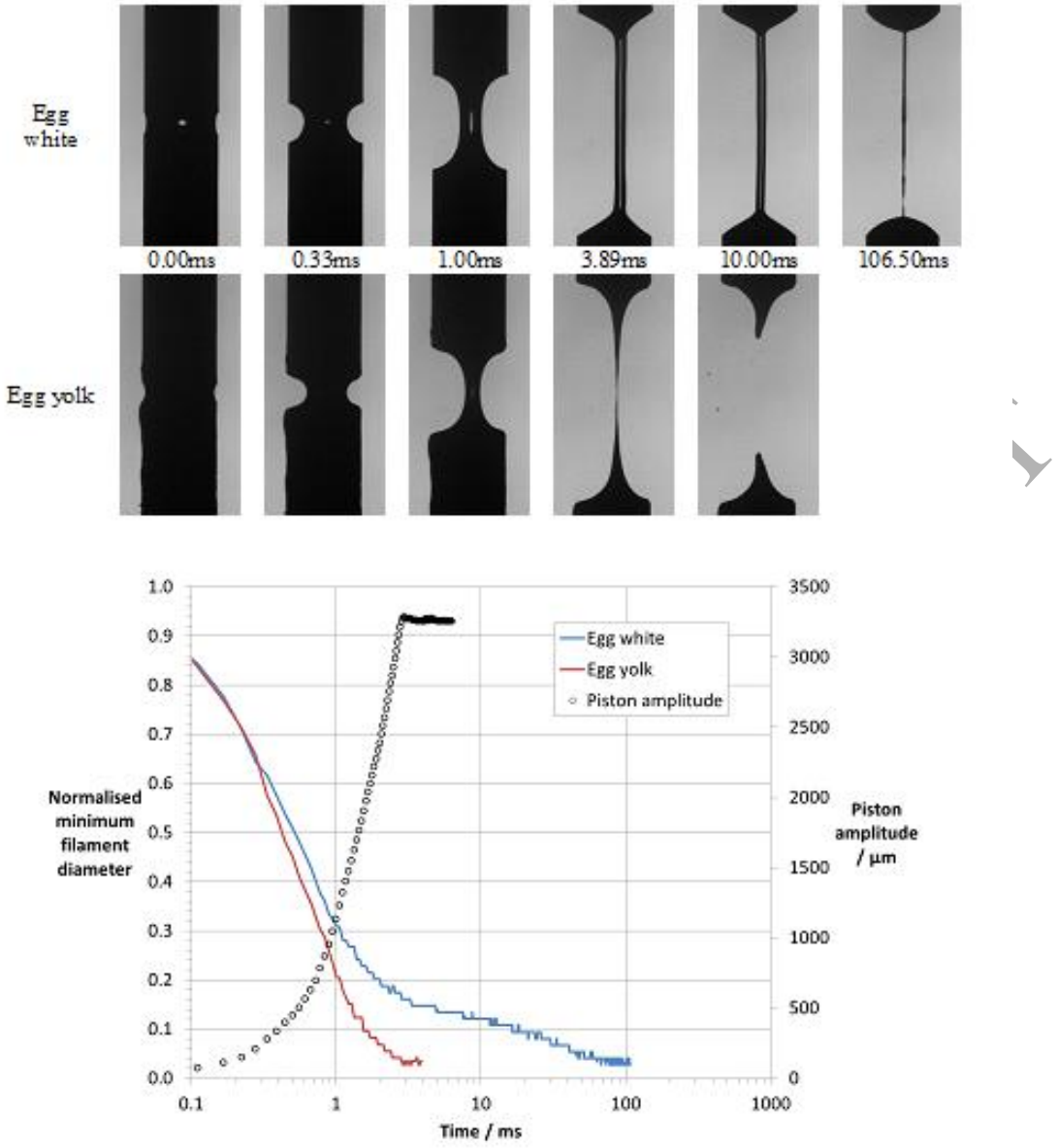

***Figure 6**. Photographs, displacement and minimum thickness plots for egg white and egg yolk. Piston diameter = 1.2 mm, initial gap = 0.34 mm, combined separation speed = 1.0 m s^{-1}.*

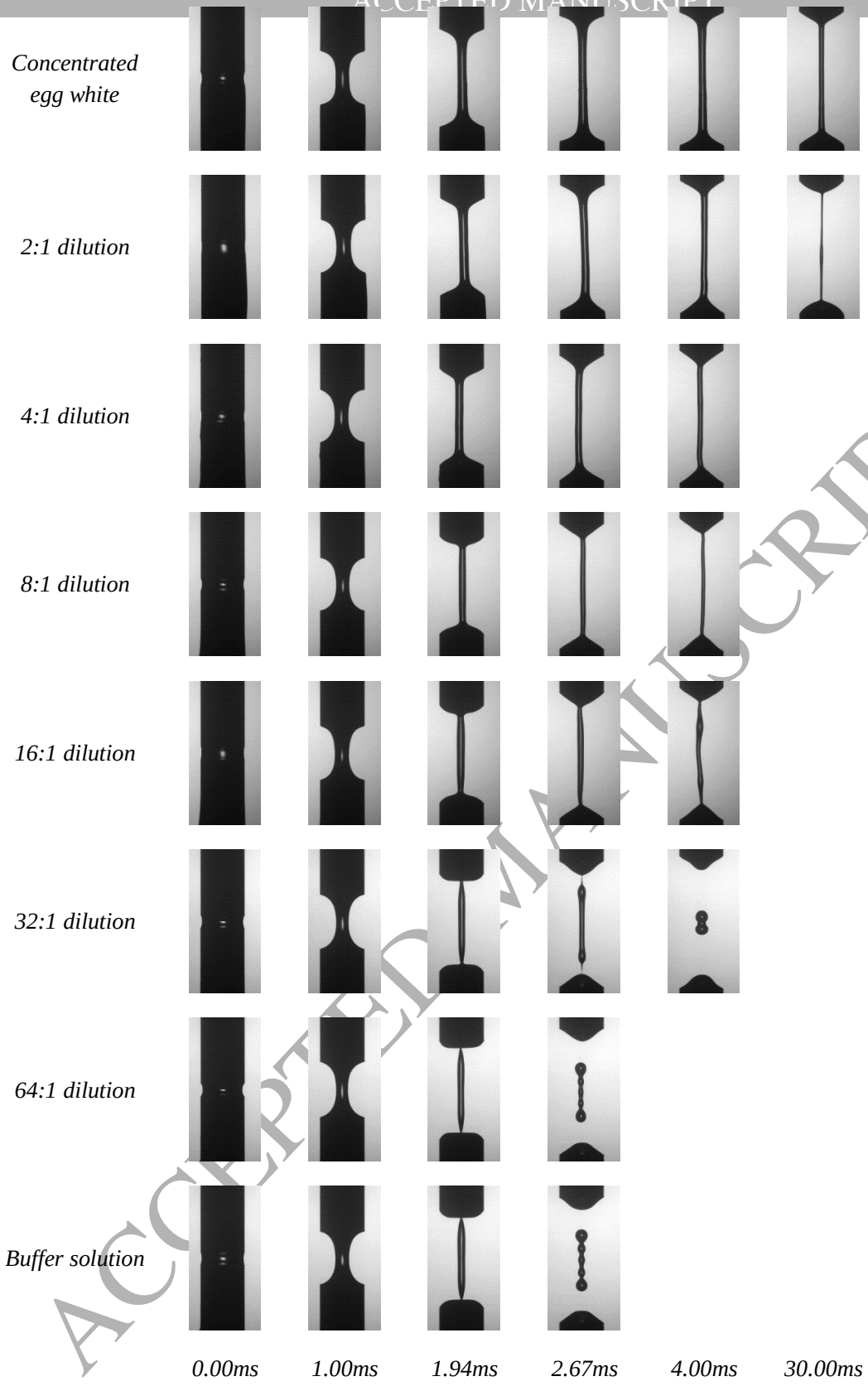

Figure 7. *Photographs for egg white diluted in PBS buffer. Dilution ratios are shown in volume basis. Piston diameter = 1.2 mm, initial gap = 0.35 mm, combined separation speed = 1.0 ms^{-1}.*

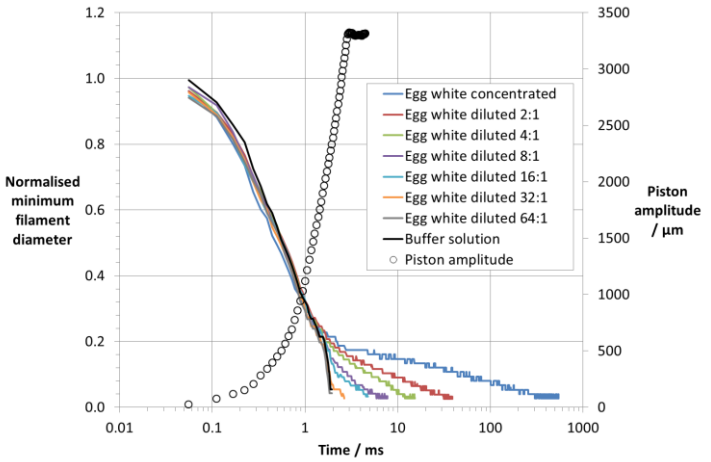

Figure 8. *Displacement and minimum thickness plots for egg white diluted in PBS buffer. Piston diameter = 1.2mm, initial gap = 0.35 mm, combined separation speed = 1.0 m s^{-1}.*

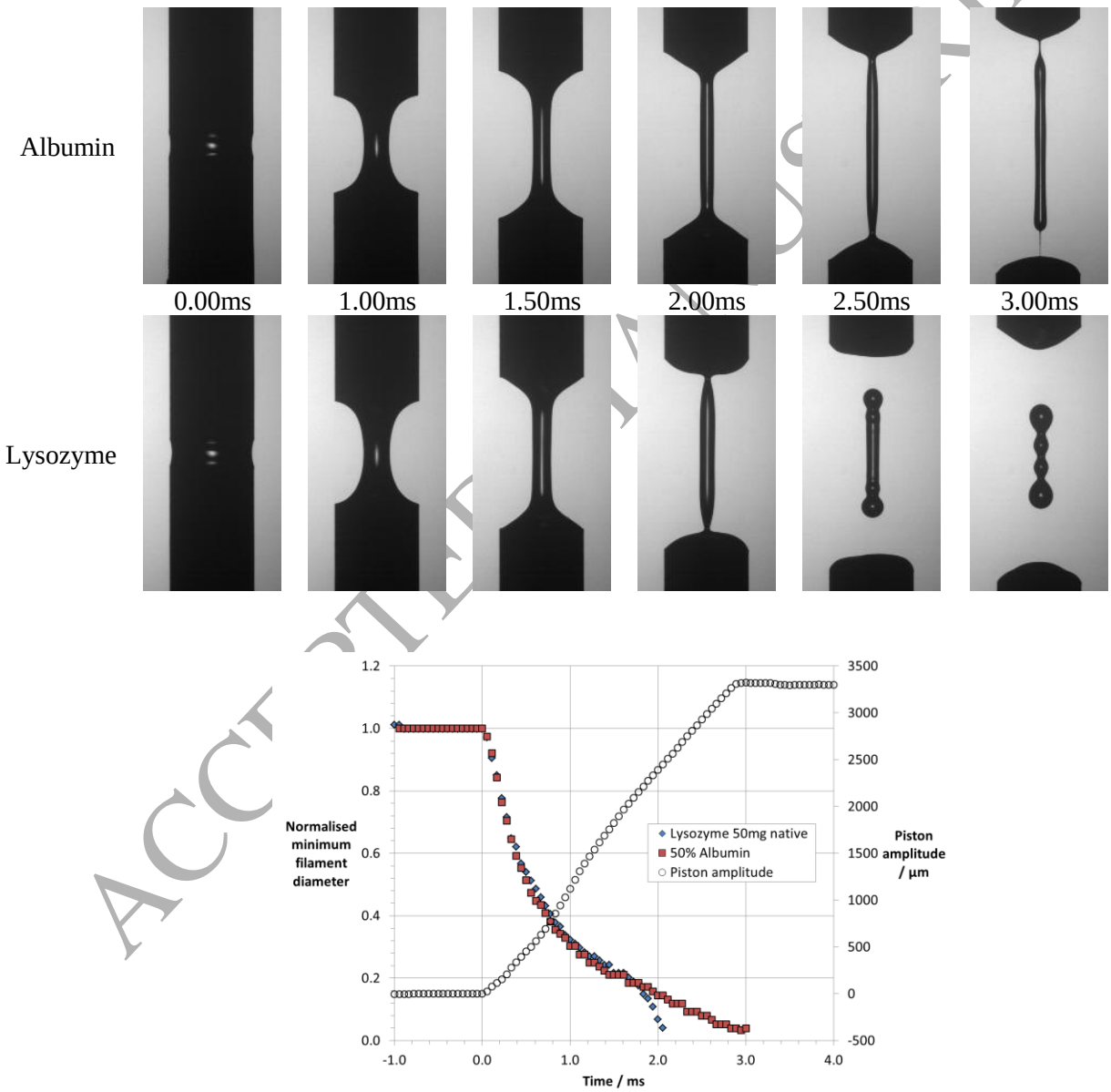

Figure 9. *Photographs, displacement and, minimum thickness plots for suspension of 50% w/w albumin and 50mg/ml of native lysozyme in BPS buffer. Piston diameter = 1.2mm, initial gap = 0.35 mm, combined separation speed = 1 m s^{-1}.*

3.4 Yield stress fluids

The final two fluids tested were everyday household foodstuffs with yields stress characteristics and Bohlin rheometer stress sweeps for both Heinz Tomato Ketchup and Hellmann's Mayonnaise are given in Appendix A of this paper. The rheology of these two fluids is complex; however from the data presented, an approximate yield stress of 20 Pa can be identified for the tomato ketchup and 100 Pa for the mayonnaise.

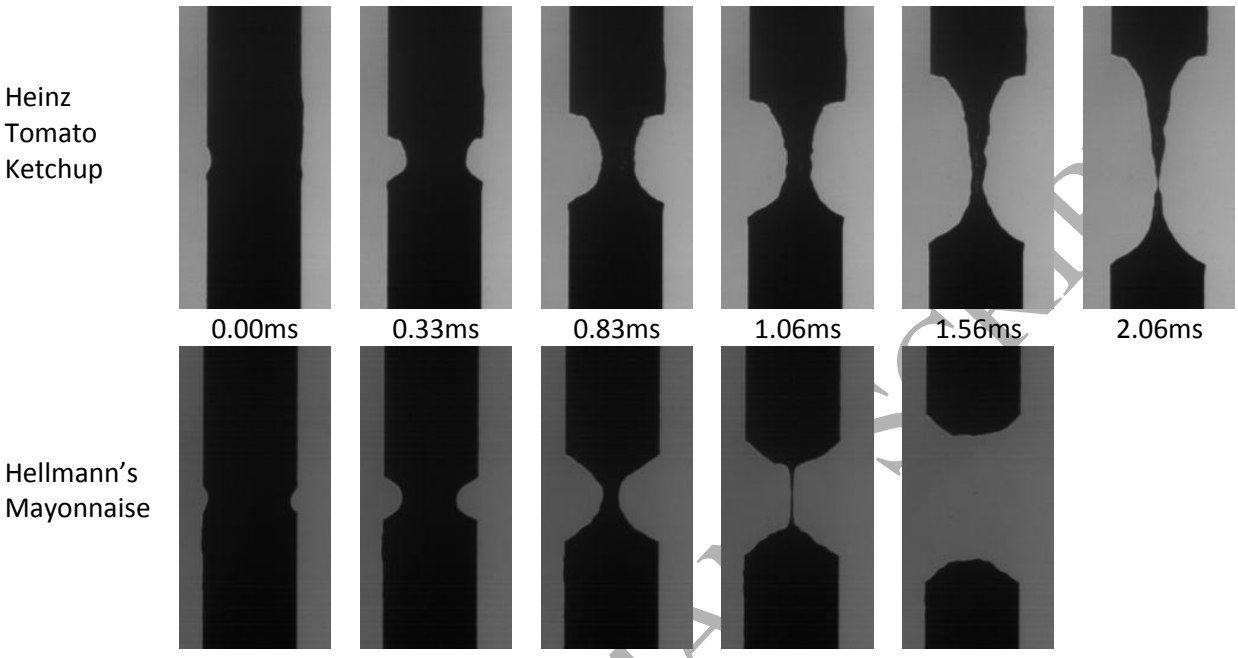

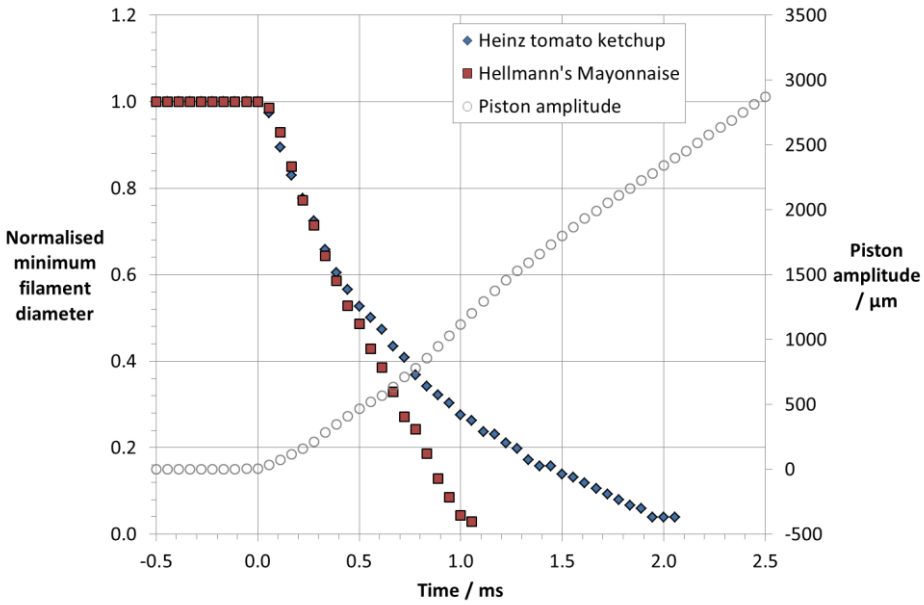

Figure 10. *Photographs, piston displacement and minimum thickness plots as a function of time for Heinz Tomato Ketchup and Hellmann's Mayonnaise. Piston diameter =1.2mm, initial gap =0.35mm, combined separation speed = 1 m* s^{-1}

Figure 10 shows both photographs and normalised diameter time change plots for tomato ketchup and mayonnaise and it can be seen that both are clearly very different in deformation and breakup to the Newtonian or polymer based fluids that have been tested before. There are however some similarities to the deformation profile observed for the egg yolk and the overall deformation behaviour appears to be that of a yield stress fluid. Once again the initial sub ms universal "wineglass" deformation profile is seen, however subsequently there is rapid thinning during the stretch period followed by necking and then "ductile fracture". The yield stress of mayonnaise is a factor of five greater than that of the Tomato Ketchup and this probably explains the observed result that the mayonnaise fractures at an earlier stretch time than the tomato ketchup, although both fracture during the stretching period of the deformation.

4. Modelling of deformation profiles.

For all the fluids tested it was noted that the very early stages of the observed deformation profiles appeared to have a very similar "wineglass" shape and this similarity is supported in Figure 11 for a range of fluids where the experimental centre line profile diameter is plotted as a function of time. It can be seen from the figure that for approximately the first 20% of the diameter decrease, all the fluids follow a very similar path. In this early time region, the deformation profile appears to be independent of the fluid rheology and this was tested by comparing the results with a simple mass balance equation derived in Appendix A that assumes an evolving parabolic profile pinned at the ends of the moving piston. This analytic parabolic equation is also plotted on Figure 11 and it can be seen that for the early time deformation behaviour, the fit is reasonably good. For later times, below a deformation ratio, (defined as the ratio of initial diameter to subsequent centre line diameter) of about 0.8, different fluids behaved in very different ways and this is where the rheology, surface tension and possibly inertia all play a part in the resulting deformation and break up.

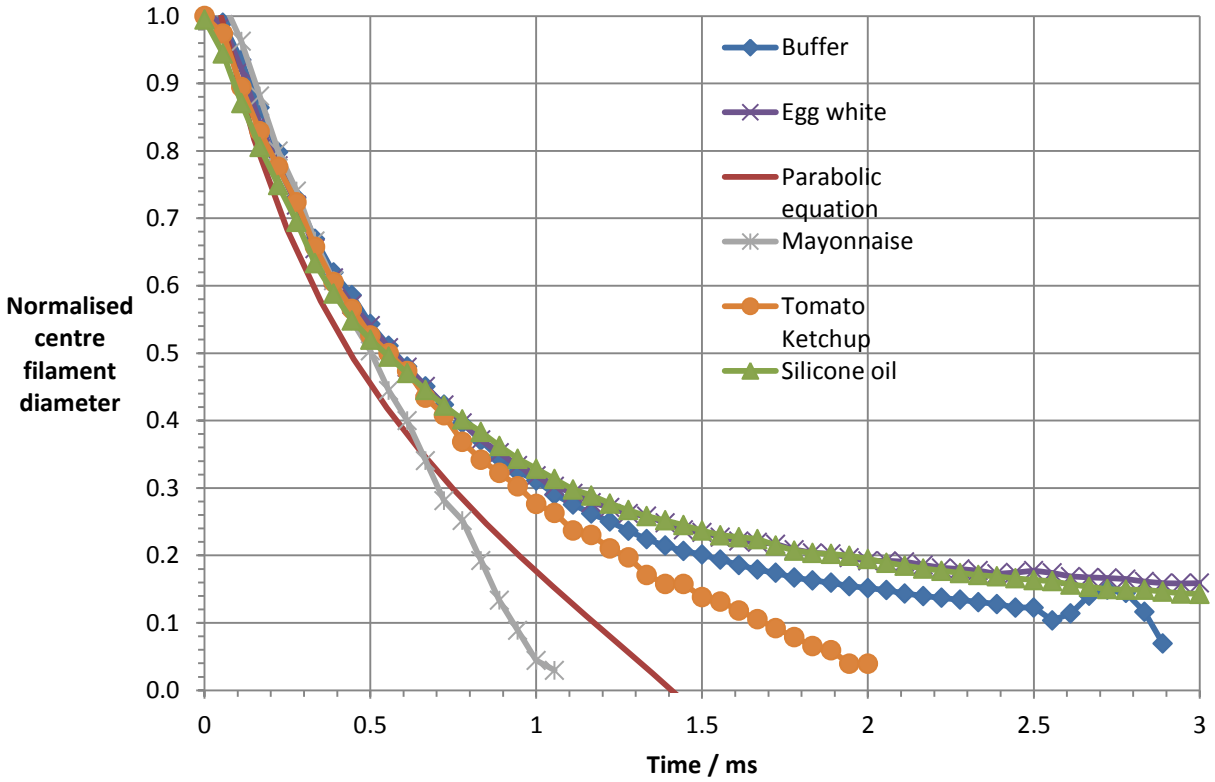

Figure 11 *Graph of normalised centre diameter as a function of time for the analytic parabolic equation and for the experimental, buffer solution, Silicone oil, Hellman's Mayonnaise, Heinz Tomato Ketchup and egg white.*

A limited amount of numerical simulation for the whole observed HB4 deformation profiles time evolution has been carried out in order to demonstrate that modelling of the whole deformation profile and breakup is possible. There were however situations such as the yield stress fluids where a full simulation is currently not possible. Using the procedure fully described in Tembely et al [30], a 1D numerical simulation for both a Newtonian fluid and also the monodisperse polystyrene solution has been compared with experimental results. A viscosity of 1.03 mPas and surface tension of 69.5 mN/m was chosen to match the properties of the buffer solution and a comparison of the normalised centre line diameter decay is shown in Figure 12 as a one position measure of behaviour. The agreement between simulation and experiment is impressive up to the point of end pinching; however the 1D simulation is unable to follow events after end pinching has occurred at 1.83 ms. The simulation does show the experimentally observed development of end pinching separation as shown in a later Figure 14c up to the point of pinch off. For the monodisperse polystyrene solution the same rheological data and model reported in Tembely et al [30] was used to compare the HB4 experimental results and the simulation results for the centre line is shown for the HB4 input boundary conditions in Figure 13. Again the simulation results follow the experimental centre line curve reasonably well and both results give confidence that Newtonian and Polymer responses can be successfully modelled. We have not yet however attempted to model the yield stress type fluid response.

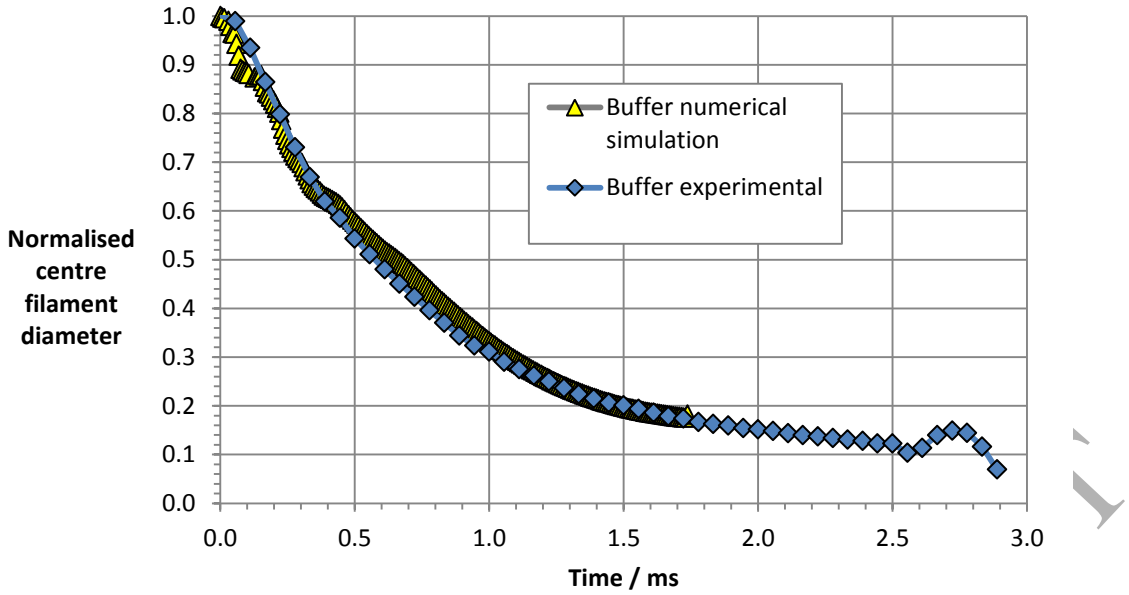

***Figure 12**. Experimental centre line buffer solution decay curve and 1D numerical simulation. Single piston velocity V_p=0.5 m s^{-1}, half starting displacement l_0 = 0.175 mm. A viscosity of 1.03 mPas and surface tension of 69.5 mN/m was used for the numerical solution*

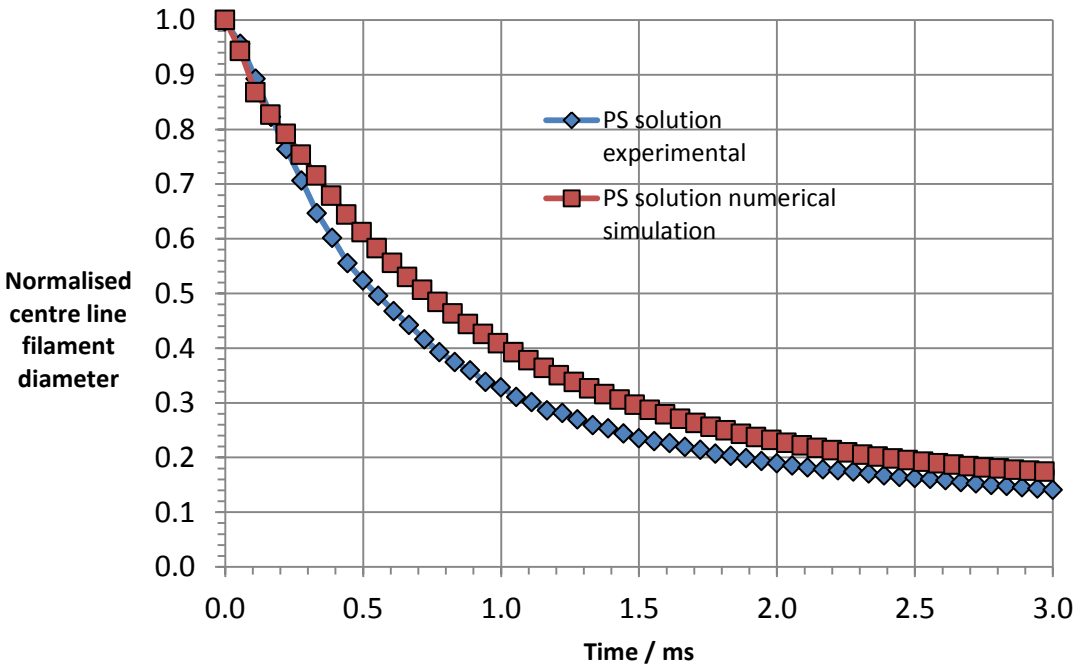

***Figure 13**. Experimental centre line polystyrene solution decay curve, with matching 1D numerical simulation. Single piston velocity V_p=0.5 m s^{-1}, half starting displacement l_0 = 0.175 mm. Rheological and physical parameters used in the simulation are given in Tembely et al [28]*

Finally the examples of the whole profile evolution for the Newtonian buffer solution is shown in Figure 14. The experimental sequence is shown in the a) series of photographs up to the point of end pinching break up at 1.83 ms which is before the pistons have stopped moving. The b) series of profiles give the form for the analytic parabolic equation and this shows that at early times there is a good match with experiment; however at later times the decay is much faster than experimentally observed profile and the analytic parabolic equation has a zero diameter cut off at

1.41 ms, which is well before the experimentally observed break up. The c) series of profiles represent the 1D numerical simulation and here it can be seen that the profiles follow both early and later times. In particular the simulation is able to predict the end pinch separation point with good accuracy.

A potential way forward to extract rheological parameters from results of the type shown in this paper is to match simulations with the full time dependent experimentally observed deformation

And breakup profiles. If the matching is good, then the both the simulation constitutive equation and the rheological parameters including the value of surface tension that have been used are valid for the particular experimental test. Alternative approaches to extracting rheological data, in particular transient extensional viscosities, exist for filament stretching and relaxation experiments (see for example refs [1,2,3 and 5]), however some of the complex deformation profiles and observed break up behaviour reported in this paper make analytic interpretation difficult.

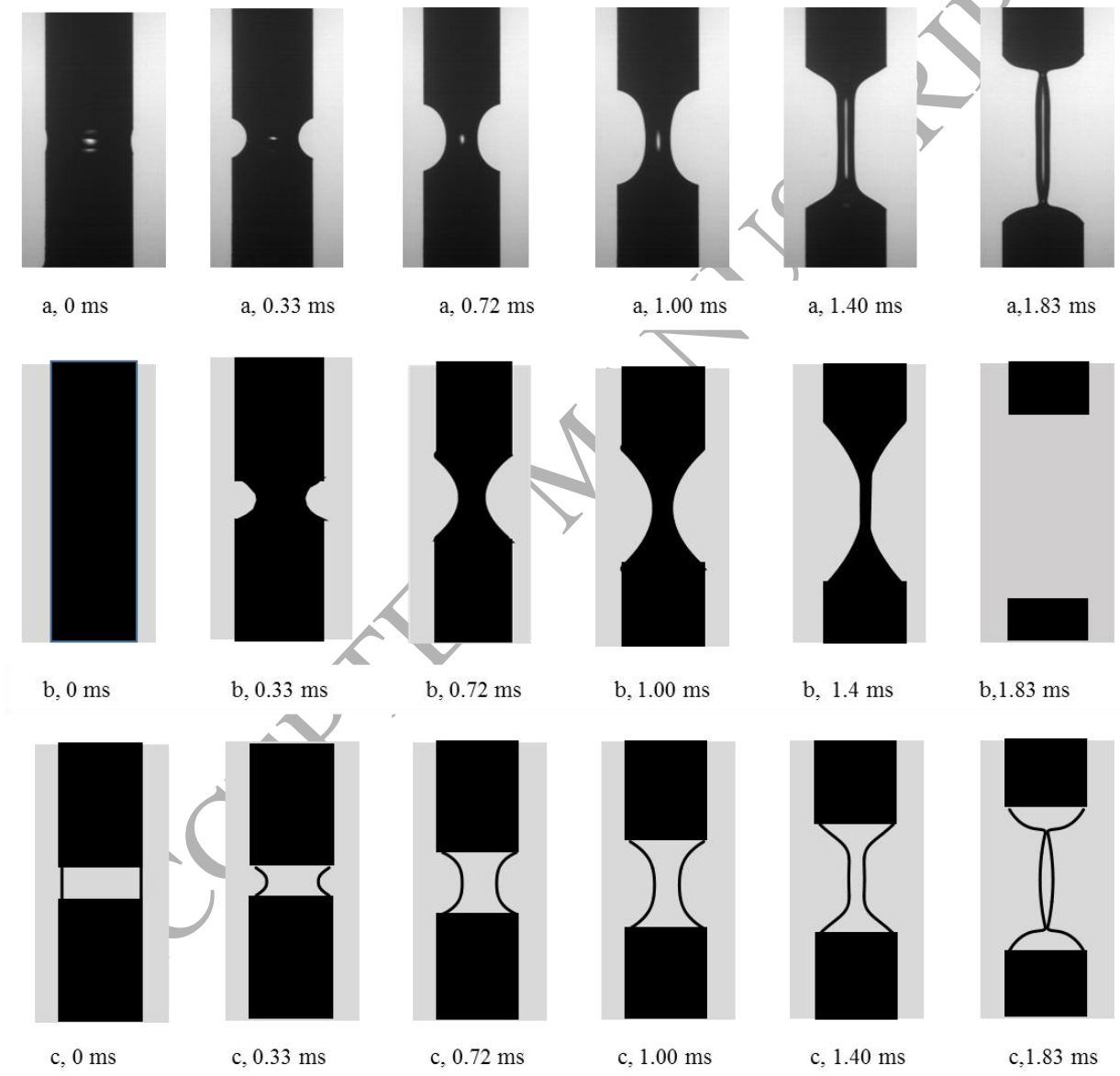

Figure 14*. a) Experimental PBS buffer, b) analytic parabolic, c) 1D numerical simulation, profiles of filament formation at a set of selected times***.**

5. Conclusions

This paper has described and shown proof of concept for a new high speed HB4 Trimaster filament stretching apparatus that is capable of producing very high extensional strain rate deformation and where a range of fluids that have been tested show very different Non Newtonian deformation profiles and break up behavior. The results from the HB4, presented for the first time in this paper, show a considerable diversity in deformation and breakup and provides insight on both aspects.

In the past, piston stretching devices have usually been associated with the measurement of extensional viscosity parameters and the HB4 could be used for this task with suitable selection of fluid viscosity and operating conditions; however this paper focusses on providing information and insight into the way very high extensional strain rates effect deformation and breakup for fluids with different rheologies.

Surprisingly the first sub ms "wine glass" deformation profiles were found to be independent of viscosity and rheology and it was discovered that this could be modelled using a simple quadratic mass balance equation. Subsequent deformation and breakup was however found to be very sensitive to fluid type and this is summarized below.

- **Newtonian fluids.**
  Moderate viscosity Newtonians (492 mPas) fluids deformed during stretching and then capillary thinned after the cessation of piston movement. The capillary thinning followed a linear kinetic which has been measured and modelled by others [11,12,13]. The low viscosity Newtonian (1.03 mPas) deformed and broke up during the stretching period. Breakup occurred by an end pinching mechanism that was very different from the higher viscosity progressive capillary thinning and numerical simulations reported in this paper was able to reproduce the end pinching effect.
- **Polymer solution.**
  The monodisperse viscoelastic polystyrene solution (base viscosity 15.3 mPas) remained intact during stretching and continued to filament thin after the cessation of piston movement. Thinning behaviour was similar to that previously reported for lower stretching conditions [19,20] and numerical simulation reported in this paper was able to capture the observed experimental results.
- **Protein Solutions**.
  Although high molecular weight biological polymers; both albumin and native lysozyme solutions showed little or no deviation from Newtonian behaviour, suggesting that polymer chain stretching had not occurred during stretching even at the applied very high extensional strain rates. The egg white and yolk did show striking effects. The egg yolk showed early break up behaviour before piston cessation in a similar way to the yield stress fluids, whereas the egg white showed polymeric initial long relaxation thinning after piston cessation and with progressive and associated viscosity reduction dilution, breakup became more Newtonian and eventually occurred in a similar way to the Newtonian Buffer with end pinching breakup occurring before piston cessation.
- **Yield stress fluids**.
  Two well-known foodstuffs, tomato ketchup and mayonnaise showed a remarkably different stretch and breakup behaviour to other fluids tested. These yield stress fluids rapidly deformed at the high stretch rates and breakup occurred at the early stage of stretching. Currently there is no matching numerical simulation available to compare with these experimental results.

These findings collectively provide experimental observations that have previously not been possible to make. The results show that different viscosities and rheologies can have a profound effect on breakup mechanisms moving from end pinching during piston movement to progressive thinning after piston cessation. The paper has shown that in some cases numerical modelling can successfully describe events however, particularly in the case of yield stress fluids, new numerical tools need to be developed to describe the processes. Molecular models do exist for

polymeric fluids see for example [31], however again, more advanced molecular mechanistic models will need to be created to for example describe both the tested yield stress fluids, egg white and yolk.

References.

[1] Anna, S. L., G. H. McKinley, D. A. Nguyen, T. Sridhar, S. J. Muller, J. Huang, and D. F. James,
‘‘An inter-laboratory comparison of measurements from filament-stretching rheometers using common test fluids,’’ J. Rheology. 45, 83–114 (2001).

[2] McKinley, G. H.,
“Visco-elastic-capillary thinning and break-up of complex fluid,” in Rheology Reviews 2005, (The British Society of Rheology, 2005), pp. 1–48.

[3] James, D.F and M. Pouran “Droplet formation in quickly stretched liquid filaments,” Rheologica Acta 48, 6, 611–624 (2009)

[4] Stone, H.A
“Dynamics of drop deformation and breakup in viscous fluids,”
Annual Review of Fluid Mechanics 26(1):65-102, (2003)

[5] James. D.J. and K. Walters,
“A critical appraisal of available methods for the measurement of extensional properties of mobile systems”, in: A.A. Collyer (Ed.), Techniques in Rheological Measurement SE – 2, Springer, Netherlands, 33–53. (1993).

[6] Keshavarz. B., V. Sharma., E. C. Houze., M. R. Koerner,, J. R. Moore., P. M. Cotts. , P. Threlfall-Holmes and G. H. McKinley,
“Studying the effects of elongational properties on atomization of weakly viscoelastic solutions using Rayleigh Ohnesorge Jetting Extensional Rheometry (ROJER),”
J. Non-Newtonian Fluid Mechanics. 222, 171-189 (2014).

[7] Crowley,D.G., F.C.Frank, M.R.Mackley and R.C.Stephenson
“Localised flow birefringence of polyethylene oxide solutions in a four roll mill. “
Journal of Polymer Science A2, 14, 1111-1119 (1976).

[8] Mackley, M.R. and A. Keller,
“Flow induced polymer chain extension and its relationship to fibrous crystallization,”
Phil. Trans. Royal Soc. (Lond.) 278, 29-66 (1975).

[9] McKinley, G. H., and T. Sridhar,
"Filament stretching rheometry of complex fluids,"
Annual. Rev. Fluid Mech. 34, 375–415 (2002).

[10] Bazilevsky, A. V., V. M. Entov, and A. N. Rozhkov,
"Liquid filament microrheometer and some of its applications", In Third European Rheology Conference, edited by D. R. Oliver (Elsevier Applied Science, London and New York, 1990), pp. 41–43.

[11] Anna, S. L., and G. H. McKinley,
"Elasto-capillary thinning and breakup of model elastic liquids,"
J. Rheology. **45**, 115–138 (2001).

[12] Entov,V.M., and E.J. Hinch,
"Effect of a spectrum of relaxation times on the capillary thinning of a filament of elastic liquid,"
Journal of Non Newtonian Fluid Mechanics.72.1, 31–53 (1997).

[13] Liang, R. F., and M. R. Mackley,
"Rheological characterisation of the time and strain dependence for polyisobutylene solutions,"

J. Non-Newtonian Fluid Mech. **52**, 387–405 (1994).

[14] Clasen, C., and J.P.Rothstein,
"The effect of step stretch parameters on capillary breakup extensional rheology (Caber) measurements,"
Rheo Acta. 48, 625- 639 (2009).

[15] Yao, M. M., G.H. McKinley, and B. Debbaut,
"Extensional deformation, stress relaxation and necking failure of viscoelastic filaments,"
J. Non-Newtonian Fluid Mech. 79, 469-501 (1998).

[16] Cooper-White, J.J., J.E.Fagan, V. Tirtaatmadja, D.R.Lester, and D.V. Boger,
"Drop formation dynamics of constant low-viscosity, elastic fluids,"
J Non-Newtonian Fluid Mech. 106, 29–59 (2002).

[17] Hoath, S.D,
"Fundamentals of Ink Jet Printing" Wiley-VCH (2016)

[18] Vadillo, D. C. , M. Tembely, N.F. Morrison, O. G. Harlen, and M. R. Mackley,
"The matching of polymer solution fast filament stretching, relaxation, and breakup experimental results with 1D and 2D numerical viscoelastic simulation,"
J. Rheology. 56, 1491-1516 (2012).

[19] Rodd, L.E., T.P. Scott., J.J. Cooper-White and G.H. McKinley,
"Capillary break-up rheometry of low-viscosity elastic fluids,"
Appl. Rheol. 15 (1) 12–27. (2005).

[20] Vadillo, D. C., T. R. Tuladhar, A. C. Mulji, S. Jung, S. D. Hoath, and M. R. Mackley,
"Evaluation of the inkjet fluid's performance using the 'Cambridge Trimaster' filament stretch and break-up device," J.
Rheology. 54(2), 261–282 (2010).

[21] Cardinaels, R., J.Van de Velde, W. Mathues, P. Van Liedekerke, and P. Moldenaers, "A rheological characterisation of liquid egg albumen,"
InsideFood Symposium, 9-12 April 2013, Leuven, Belgium 1-6 (2013).

[22] Tung, M.A., J. F. Richards., B.C. Morrison, and E. L.Watson.
"Rheology of fresh, aged and gamma-irradiated egg white,"
J. Food Sci. 35, 872-874 (1970).

[23] Kemps, B.J., F.R. Bamelis, K. Mertens, E.M. Decuypere, J.G. De Baerdemaeker, and B. De Ketelaere,
"The Assessment of viscosity measurements on the albumen of consumption eggs as an indicator for freshness",
Poultry Science. 89, 2699-2703 (2010).

[24] Shenstone, F.S.,
"The gross composition, chemistry and physico-chemical basis of organization of the yolk and white," in T.C. Carter (Ed.) Egg quality A study of the hen's egg (pp. 26-58)

Oliver & Boyd, Edinburgh. (1968).

[25] Huopalahti, R., R. Lopez-Fandino, M.Anton, and R. Schade,
"Bioactive egg compounds", Pub, Springer, Berlin Heidelberg. (2007).

[26] Telis-Romero,J., C.E.P. Thomaz., M. Bernardi., V.R.N. Telis and A.L. Gabas "Rheological properties and fluid dynamics of egg yolk"
Journal of Food Engineering 74, 191–197 (2006).

[27] Niedzwiedz.K., Buggisch. H., and N. Willenbacher
"Extensional rheology of concentrated emulsions as probed by capillary breakup elongational rheometry (CaBER),"
Rheol Acta 49, 1103-1116 (2010).

[28] Sharma. V., A. Jaishankar., Y.C. Wang and G. H. McKinley
"Rheology of globular proteins: apparent yield stress, high shear rate viscosity and interfacial viscoelasticity of bovine serum albumin solutions,"
Soft Matter 7, 5150-5160 (2011).

[29] Castellanos. M.M., Pathak.J.A, and Ralph H. Colby
"Both protein adsorption and aggregation contribute to shear yielding and viscosity increase in protein solutions,"
Soft Matter, 10, 122–131 (2014).

[30] Tembely, M., D. C. Vadillo, M. R. Mackley, and A. Soucemarianadin,
"The matching of a "one-dimensional" numerical simulation and experiment results for low viscosity Newtonian and non-Newtonian fluids during fast filament stretching and subsequent break-up,"
J. Rheology. 56, 159–184 (2012).

[31] Larson,R.G., "Constitutive equations for polymer melts and solutions" Butterworths (2013)

Acknowledgements.
We would like to thank the EPSRC and the associated Cambridge Industrial Ink Jet consortium for encouragement and financial support of this project. We also thank Mrs Julie Ferguson for the supply of the fresh, free range hens egg.

Appendix A

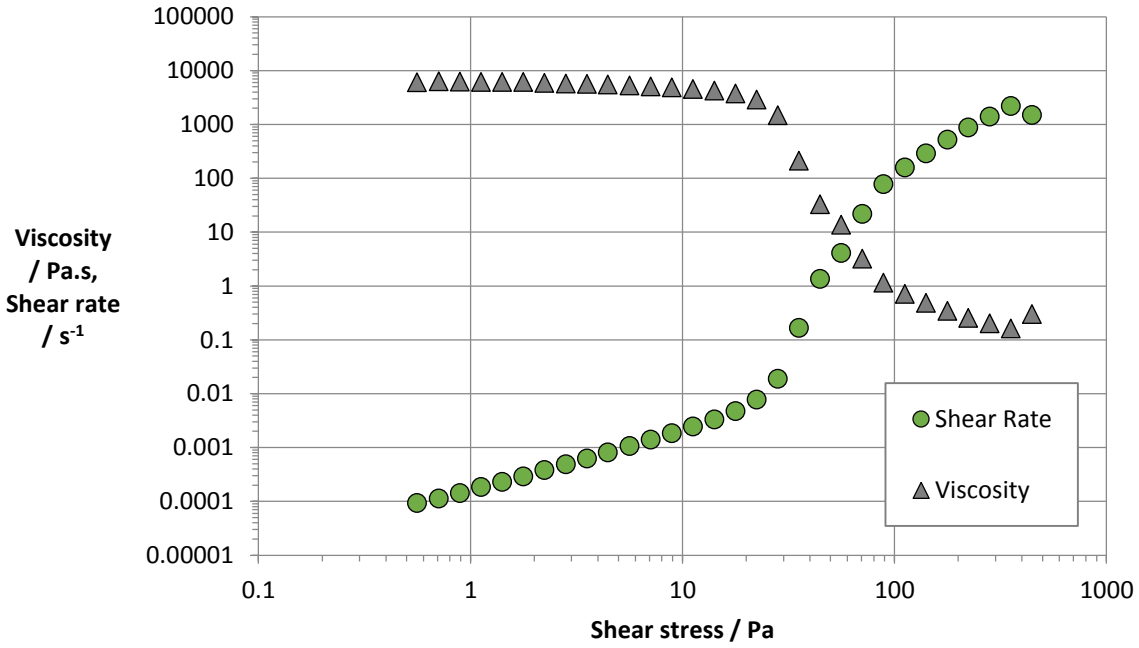

15 a

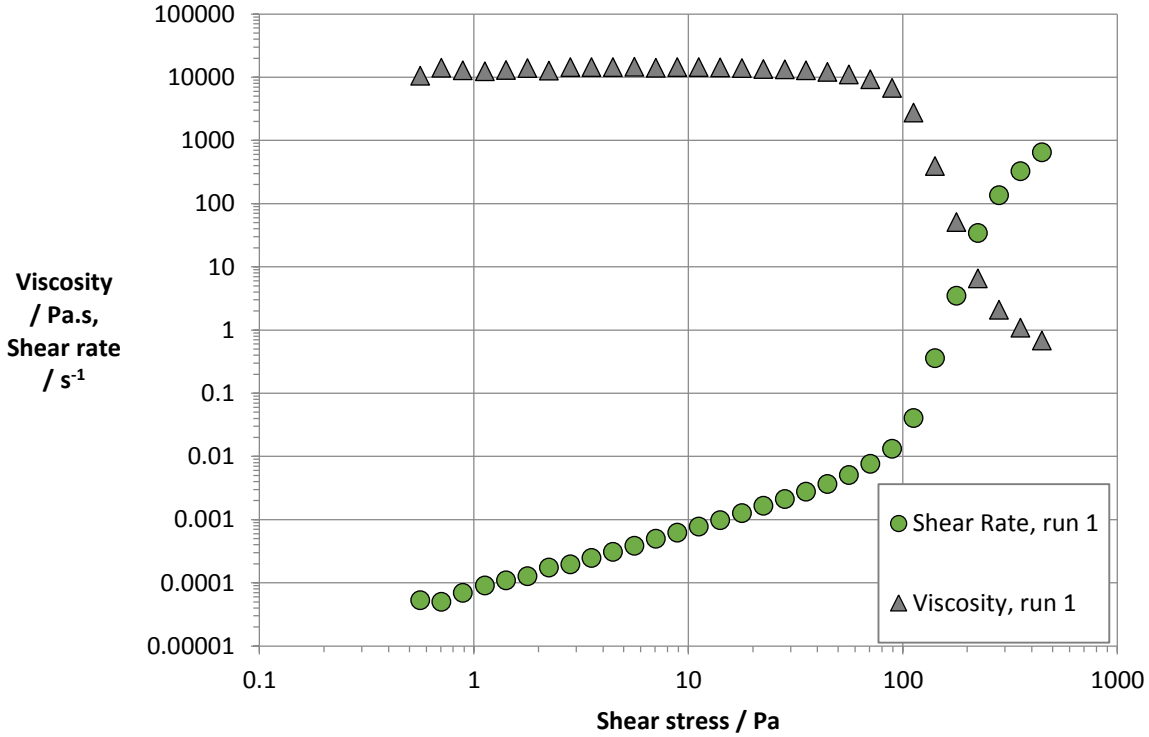

15 b

Figure 15. *Bohlin controlled stress sweeps for a) Heinz Tomato Ketchup and b) Hellmann's Mayonnaise.*

Appendix B

Volume balance equation for filament stretching, combined with parabolic profile assumption.

Figure 16 shows the initial and subsequent boundary conditions for axi and centro symmetric filament stretching with a constant single piston velocity u =V_p, initial half piston separation l_o and initial cylindrical fluid diameter of r_o.

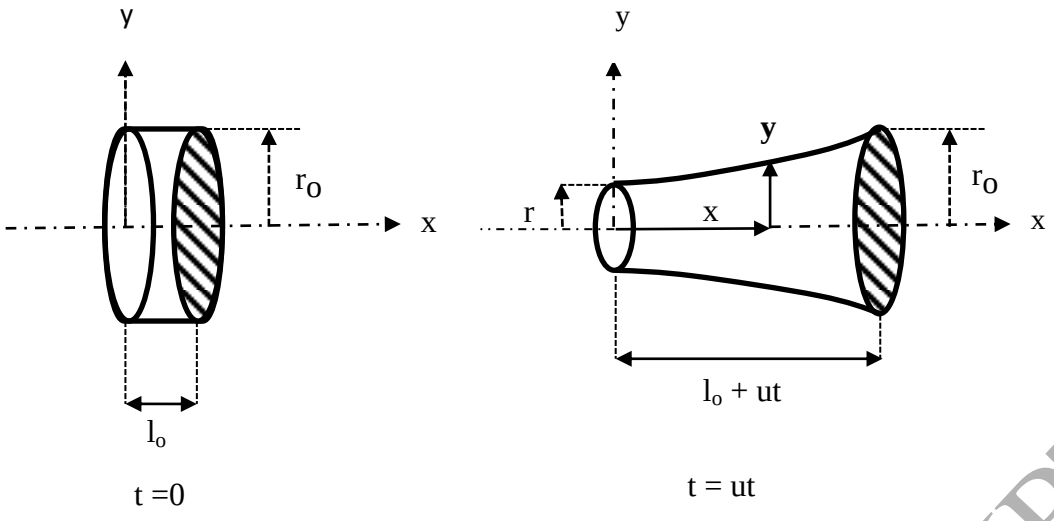

***Figure 16**. schematic of filament stretching.*

Parabolic profile.

At t = 0 x = l_0 , y = r_0
At t = t x= l_0 + ut , y = r_o , where u = piston velocity
Let y = r at x = 0
Assume parabolic profile $y = r + \alpha x^2$
then $r_o = r + \alpha (l_o + ut)^2$
so $\alpha = \frac{(r_o - r)a^2}{(l_o+ut)^2}$
then $y = r + \frac{(r_o - r)}{(l_o+ut)^2} x^2$ *(B1)*
Volume balance

$$\pi r_o^2 l_o = \pi \int_o^{(l_o+ut)} y^2 \, dx \qquad (B2)$$

Combining equations *(B1)* and *(B2) and integrating* yields centre line radius *r*, where the numerical coefficients result from the integration and are not adjustable parameters.

$$\frac{r}{r_o} = -0.249 + 0.938\left(0.070 - 2.132\left(0.2 - \frac{l_o}{l_0+ut}\right)\right)^{1/2} \qquad (B3)$$